

# A Monotonic Algorithm for Eigenvalue Optimization in Shape Design Problems of Multi-Density Inhomogeneous Materials

Zheng-fang Zhang, Ke-wei Liang\* and Xiao-liang Cheng

*Department of Mathematics, Zhejiang University, Hangzhou 310027, China.*

Received 19 March 2009; Accepted (in revised version) 20 October 2009

Available online 15 April 2010

---

**Abstract.** Many problems in engineering shape design involve eigenvalue optimizations. The relevant difficulty is that the eigenvalues are not continuously differentiable with respect to the density. In this paper, we are interested in the case of multi-density inhomogeneous materials which minimizes the least eigenvalue. With the finite element discretization, we propose a monotonically decreasing algorithm to solve the minimization problem. Some numerical examples are provided to illustrate the efficiency of the present algorithm as well as to demonstrate its availability for the case of more than two densities. As the computations are sensitive to the choice of the discretization mesh sizes, we adopt the refined mesh strategy, whose mesh grids are 25-times of the amount used in [S. Osher and F. Santosa, *J. Comput. Phys.*, 171 (2001), pp. 272-288]. We also show the significant reduction in computational cost with the fast convergence of this algorithm.

**AMS subject classifications:** 35P15, 65K10, 74S05

**Key words:** Multi-density, inhomogeneous materials, the least eigenvalue, optimization problem, finite element method, monotonic algorithm.

---

## 1 Introduction

Consider the least eigenvalue problem of

$$\begin{aligned} -\Delta u &= \lambda \rho(x)u, & x \in \Omega, \\ u &= 0, & x \in \partial\Omega, \end{aligned} \tag{1.1}$$

---

\*Corresponding author. *Email addresses:* sophiazzf@126.com (Z. Zhang), mat1kw@zju.edu.cn (K. Liang), xiaoliangcheng@zju.edu.cn (X. Cheng)

where  $\Omega$  is a smooth, bounded and connected subset of  $R^2$ . The density  $\rho(x)$  is a piecewise-constant function

$$\rho(x)|_{\Omega_i} = \rho_i > 0, \quad i = 1, 2, \dots, m, \tag{1.2}$$

where  $0 < \rho_1 < \rho_2 < \dots < \rho_m$  are constants, and  $\Omega_i$  ( $i = 1, \dots, m$ ) are measurable subdomains of  $\Omega$  such that

$$\Omega_1 \cup \Omega_2 \cup \dots \cup \Omega_m = \Omega, \quad \Omega_i \cap \Omega_j = \emptyset \quad (i \neq j).$$

This problem is modeled in structure engineering design [1,3,4,21]. For example, a structure is assigned to support a given load, but it must be as light as possible to satisfy a compliance constraint (see [16] and therein references). Another example is to determine the shape of the vibrating membranes, which are composed of the materials with different densities (see [14, 18, 19, 23]).

Generally, such type of problems involving geometry or other constraints can be viewed as constrained optimization. For (1.1) and (1.2), we focus on the constraints of  $\{\Omega_i\}_{i=1}^m$ . Theoretically, we do not assume any topology on  $\Omega_i$ , except its area.

$$\|\Omega_i\| = \gamma_i \|\Omega\|, \quad i = 1, \dots, m, \tag{1.3}$$

where  $\|\Omega_i\|$  is the area of  $\Omega_i$ , all  $\gamma_i$  are given and

$$\gamma_1 + \gamma_2 + \dots + \gamma_m = 1.$$

From the weak formula of (1.1)

$$\int_{\Omega} \nabla u \cdot \nabla v dx = \lambda \int_{\Omega} \rho(x) u v dx, \quad \forall v \in H_0^1(\Omega), \tag{1.4}$$

there indeed exists a sequence of nontrivial eigenvalues [6]

$$0 < \lambda_1(\Omega, \rho) \leq \lambda_2(\Omega, \rho) \leq \dots \rightarrow \infty.$$

The optimization problems related to the eigenvalues  $\lambda_1(\Omega, \rho)$  and  $\lambda_2(\Omega, \rho)$  can be (i)  $\min \lambda_1$ ; (ii)  $\max \lambda_1$ ; (iii)  $\max(\lambda_2 - \lambda_1)$ , with the conditions (1.2) and (1.3).

In this paper, we only consider the optimal problem (i). That is, how to seek the sets  $\{\Omega_i\}$  ( $i = 1, \dots, m$ ) such that the least eigenvalue  $\lambda_1$  of the problem (1.1)-(1.2) is minimizing. This problem also arises from the shape design of multi-density inhomogeneous drum (see [7, 16]). Recalling the weak formula (1.4), we get the associated variational characterization

$$\lambda_1(\rho(x)) = \min_{u \in H_0^1(\Omega)} \frac{\int_{\Omega} |\nabla u|^2 dx}{\int_{\Omega} \rho(x) u^2 dx}. \tag{1.5}$$

In order to shed the numerator in (1.5), we denote by  $H_1^1(\Omega)$  the class of  $H_0^1(\Omega)$  functions with  $H^1$  seminorm 1. The optimization problem (1.5) can be simplified as

$$\lambda_1(\rho) = \min_{u \in H_1^1(\Omega)} \frac{1}{\mathcal{R}(u, \rho)}, \tag{1.6}$$

where

$$\mathcal{R}(u, \rho) = \int_{\Omega} \rho(x) u^2 dx.$$

The above expression illustrates the minimum is closely linked to  $\rho$ . Therefore, an equivalent formula of the problem (i) is

$$\min_{\rho \in ad_{\gamma}(\Omega)} \lambda_1(\rho), \tag{1.7}$$

where

$$ad_{\gamma}(\Omega) = \left\{ \sum_{i=1}^m \rho_i \chi_i(x) : \Omega_i \subseteq \Omega, \|\Omega_i\| = \gamma_i \|\Omega\|, \sum_{i=1}^m \gamma_i = 1 \text{ and } \gamma_i > 0, i = 1, \dots, m \right\}$$

and  $\chi_i$  is the characteristic function of  $\Omega_i, i = 1, 2, \dots, m,$

$$\chi_i(x) = \begin{cases} 1, & x \in \Omega_i, \\ 0, & x \in \Omega \setminus \Omega_i. \end{cases}$$

Typically, if  $\rho \equiv \rho_1$  and the area of  $\Omega$  is fixed, the optimization problem (i) is then  $\min_{\|\Omega\|=A} \lambda_1(\Omega)$ . This problem comes first from the homogenous drum and an argument is gotten in [2] that the appropriate disk is the minimizer. The mathematical proof can be found in [10,12]. A numerical algorithm is also presented in [20] to compute eigenvalues and eigenfunctions of this problem, even for the case of arbitrary bounded plane regions  $\Omega$ .

For the case of  $m = 2$ , the density  $\rho$  is chosen from the class

$$ad(\Omega) = \left\{ \rho_1 \chi_1(x) + \rho_2 \chi_2(x) : \Omega_i \subseteq \Omega, \|\Omega_i\| = \gamma_i \|\Omega\|, \gamma_1 + \gamma_2 = 1 \text{ and } \gamma_i > 0, i = 1, 2 \right\}.$$

The problem (i) over  $ad(\Omega)$  has been considered in [13] where  $\Omega$  is a disk. In order to obtain the minimum, the material with high density has to be placed in the center of the disk and the remaining annulus is filled by the low density material. Moreover, this argument is strictly positive in one-dimensional case. The same problem has been studied in [7] for the case of high-dimensional  $\Omega$ . The results of [7] show that the interface between the two materials occurs on a level set of the first eigenfunction. More precisely, if  $\rho \rightarrow \lambda_1(\rho)$  over  $ad(\Omega)$  attains its minimum, which is denoted by  $\check{\rho}$ , there exists a constant  $\nu > 0$  such that

$$\check{\rho} = \begin{cases} \rho_1, & \text{if } \check{u}_1(x) < \nu, \\ \rho_2, & \text{if } \check{u}_1(x) > \nu, \end{cases} \tag{1.8}$$

for almost every  $x \in \Omega$  [8].  $\check{u}_1(x)$  is the associated eigenfunction with respect to  $\lambda_1(\check{\rho})$ . Therefore, the optimal distribution of the densities is completely determined by its level set

$$\Gamma \equiv \{x \in \Omega : \check{u}(x) = \nu\}.$$

Through the computation of  $\Gamma$ , an algorithm presented in [5] can be implemented to search for the minimum.

In this paper, we consider the problem (i) in the case of the materials composed with more than two densities. In general, the eigenvalues of these problems are not continuously differentiable functions with respect to the parameter  $\rho$ . It may generate a considerable amount of computation if the semi-definite programming techniques are merely applied [9, 15]. Moreover, the unawareness of the topology of  $\Omega_i$  is a challenge to solve this problem [11]. These motivate our monotonic algorithm for problem (1.1) with generalized  $m$ . Recalling  $\mathcal{R}(u, \rho)$  defined in (1.6), we know that the key problem is to choose  $\rho$  from  $ad_\gamma(\Omega)$  such that  $\mathcal{R}$  attains its extremum. Sparked by this interesting idea, we present a monotonic decreasing sequence of  $\rho$  to search for the minimum. It is important to note that the monotonic algorithm has the similar form compared with the method of [5] in the case of  $m = 2$ . But their motivations are different. The starting point in [5] is to search the level-set line  $\Gamma$ , whereas the goal of the monotonic algorithm is to decrease  $1/\mathcal{R}(u, \rho)$ . This is the reason that the monotonic algorithm may be naturally extended to the case of  $m > 2$ . Numerical experiments will demonstrate the good performance of the monotonic algorithm for the cases of  $m \geq 2$ .

Recently, a level-set method has also presented in [16] to solve the optimal problem (1.1) with two different densities. The level-set method is composed of the level set formula [17], the variational level set calculus [25] and the projected gradient method [22]. Their approach requires the computation of the generalized eigenvalues problem at each iteration, solving the Hamilton Jacobi equations which describe the surface evolution and using level set technology to track the evolving interface. From an optimization point of view, their method is equivalent to a steepest descent method and sometimes converges slowly [11]. The numerical results in [16] confirm that the level set method reaches a stable value after around 200 iterations or more. Compared with the level set method, the monotonic algorithm converges faster and obtain a stable minimum of  $\lambda$  in fewer iterations. Furthermore, we always implement these numerical algorithms in a discrete way. Hence, choosing the discretization mesh sizes is important since the computation of the least eigenvalue  $\lambda_1$  is sensitive to it. In [16], the mesh sizes in  $x$ - and  $y$ -direction are  $\Delta x = \Delta y = 0.025$ , i.e.,  $40 \times 60$  mesh grids. In this paper, we adopt  $200 \times 300$  mesh grids which is 25-time the amount of those in [16]. The numerical results illustrate that the smaller the mesh sizes are, the smaller the minimum  $\lambda_1$  is. Especially, for the more densities case, the sensitivity to numerical results is much higher. Hence it is necessary to compute the minimum  $\lambda_1$  on the enough smaller mesh sizes. However, such approach may generally cause tremendous increases in the amount of computations as it requires accurate evaluations of eigenvalues and eigenfunctions. Nevertheless, this does not affect the monotonic algorithm too much since the algorithm still converges very fast.

The paper is organized as follows. In Section 2 we will introduce the monotonic algorithm in the discretization way. And a monotonic convergence theory is also presented there. Moreover, the algorithm is summarized in the pseudocodes. Numerical experiments will be given in Section 3.

## 2 The monotone algorithm

Based on (1.6) and (1.7), we obtain the following optimal problem of the least eigenvalue  $\check{\lambda}$

$$\check{\lambda}_1(\check{u}, \check{\rho}) = \min_{\rho \in ad_\gamma(\Omega)} \min_{u \in H_0^1(\Omega)} \frac{1}{\mathcal{R}(u, \rho)}, \tag{2.1}$$

where  $\check{u}$  and  $\check{\rho}$  are the values such that the least eigenvalue is minimized. In order to solve (2.1), we consider the application of the finite element method.

First, we divide the domain  $\Omega$  into finite elements  $\{T_j\}_{j=1}^n$  and confine the density  $\rho$  to finite-dimensional spaces. So we can assume that  $\rho$  in every element  $T_j$  is a constant  $\theta_j$ . Introducing  $\chi_{T_j}$  the characteristic function of  $T_j$ , we have

$$\rho(x) = \sum_{j=1}^n \theta_j \chi_{T_j}(x), \tag{2.2}$$

where  $\theta_j \in \{\rho_i\}_{i=1}^m$  and

$$\chi_{T_j}(x) = \begin{cases} 1, & x \in T_j, \\ 0, & \text{else.} \end{cases}$$

On the other hand, for a  $p$ -dimensional subspace of  $H_0^1(\Omega)$ , we have a set of finite element basis functions  $\{\varphi_i\}_{i=1}^p$  defined in  $\{T_j\}_{j=1}^n$ . The eigenfunction we search for has the form

$$u(x) = \sum_{i=1}^p u_i \varphi_i(x). \tag{2.3}$$

Further, let

$$U = (u_1, u_2, \dots, u_p)^T, \quad \Theta = (\theta_1, \theta_2, \dots, \theta_n)^T.$$

Then, substituting (2.3) into the weak form (1.4), we get the following  $p \times p$  eigensystem

$$KU = \Xi MU, \tag{2.4}$$

where  $K$  is the stiffness matrix

$$K_{ij} = \int_{\Omega} \nabla \varphi_i \nabla \varphi_j dx$$

and the mass matrix  $M$ ,

$$M_{ij} = \int_{\Omega} \rho(x) \varphi_i \varphi_j dx.$$

$U$  is the associated eigenvector and  $\Xi$  is one of the generalized eigenvalues of  $K$  with  $M$ . From (2.2), we note that  $M$  is dependent on  $\Theta$

$$M_{ij} = \sum_{k=1}^n \theta_k \int_{\Omega} \chi_{T_k}(x) \varphi_i \varphi_j dx = \sum_{k=1}^n \theta_k \int_{T_k} \varphi_i \varphi_j dx.$$

Denoting by  $\Xi_1(\Theta)$  the least eigenvalue of (2.4), we consider the discrete variational characterization [18]

$$\Xi_1(\Theta) = \min_{\langle KU, U \rangle = 1} \frac{1}{\mathcal{R}(U, \Theta)}, \tag{2.5}$$

where  $\mathcal{R}(U, \Theta) = \langle MU, U \rangle$ . Then the finite-dimensional optimization problem of (2.1) is

$$\min_{\Theta \in AD_\gamma} \Xi_1(\Theta), \tag{2.6}$$

where

$$AD_\gamma = \left\{ \Theta \mid \theta_j \in \{\rho_i\}_{i=1}^m, \sum_{j \in I_i} \|\mathbf{T}_j\| = \gamma_i \|\Omega\|, \sum_{i=1}^m \gamma_i = 1, i = 1, \dots, m, j = 1, \dots, n \right\} \tag{2.7}$$

and  $I_i$  is the set of index  $j$  such that  $\theta_j = \rho_i$ .

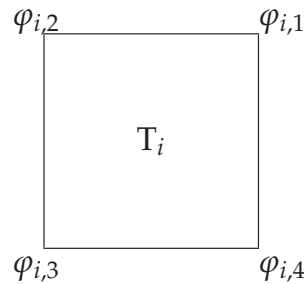


Figure 1: The rectangle element  $T_i$  and its four basis functions  $\{\varphi_{i,k}\}_{k=1}^4$ .

In this paper, we consider the rectangle finite element. For every element  $T_i$ , we have four bilinear basis functions  $\{\varphi_{i,k}\}_{k=1}^4$ , which are counter-clockwise arranged as shown in Fig. 1. Furthermore, we suppose that the components of the eigenfunction  $U$  at four nodes of  $T_i$  are  $\{u_{i,k}\}_{k=1}^4$  with respect to  $\{\varphi_{i,k}\}_{k=1}^4$ . Then  $\mathcal{R}(U, \Theta)$  is

$$\langle MU, U \rangle = \sum_{i=1}^n \theta_i \int_{T_i} \sum_{k=1}^4 \sum_{j=1}^4 \varphi_{i,k} \varphi_{i,j} u_{i,k} u_{i,j} dx.$$

Using the definitions of  $\{\varphi_{i,k}\}_{k=1}^4$ , we deduce that

$$\begin{aligned} & \int_{T_i} \sum_{k=1}^4 \sum_{j=1}^4 \varphi_{i,k} \varphi_{i,j} u_{i,k} u_{i,j} dx \\ &= \frac{\|T_i\|}{36} \left( 4u_{i,1}^2 + 4u_{i,1}u_{i,2} + 2u_{i,1}u_{i,3} + 4u_{i,1}u_{i,4} + 4u_{i,2}^2 \right. \\ & \quad \left. + 4u_{i,2}u_{i,3} + 2u_{i,2}u_{i,4} + 4u_{i,3}^2 + 4u_{i,3}u_{i,4} + 4u_{i,4}^2 \right). \end{aligned} \tag{2.8}$$

For convenience we denote by  $H_i(U)$  the integral term in the left side of (2.8) and have

$$\mathcal{R}(U, \Theta) = \sum_{i=1}^n \theta_i H_i(U). \tag{2.9}$$

Recalling (2.6), we should make a maximum of  $\mathcal{R}(U, \Theta)$  with suitable combination between  $\theta_i$  and  $H_i(U)$ ,  $i = 1, 2, \dots, n$ . Sparked by this idea, we begin with the following lemma to construct the monotone algorithm.

**Lemma 2.1.** *If  $0 < a_1 \leq a_2 \leq \dots \leq a_n$  and  $0 < b_1 \leq b_2 \leq \dots \leq b_n$ , then*

$$a_1 b_{i_1} + a_2 b_{i_2} + \dots + a_n b_{i_n} \leq a_1 b_1 + a_2 b_2 + \dots + a_n b_n$$

where  $\{i_k\}_{k=1}^n$  is any permutation of indexing set  $\mathcal{K} = \{1, 2, \dots, n\}$ .

We note that when  $\rho$  is given, the least eigenvalue  $\lambda_1$  and the associated eigenfunction  $u_1$  can be determined by (1.6). Now we consider a perturbation of  $\{\Omega_i\}_{i=1}^m$ . We (tinily) change the locations of some part of or the whole  $\{\Omega_i\}$  and denote it by  $\{\Omega_i^1\}_{i=1}^m$ , but the constrain (1.3) still holds. Then we get a new  $\rho$  defined over  $\{\Omega_i^1\}_{i=1}^m$ . And this procedure may continue. Similarly, we consider the discretization case. We adopt the uniform rectangle elements  $\{T_j\}_{j=1}^n$  over the domain  $\Omega$ , where  $\|T_j\| = \Delta x \times \Delta y$ ,  $j = 1, \dots, n$ ,  $\Delta x$  and  $\Delta y$  are the sizes of  $T_j$  in  $x$ - and  $y$ -direction respectively. If  $\Delta x$  and  $\Delta y$  are so small that  $\Omega_i$  is composed by some of  $\{T_j\}_{j=1}^n$ , the perturbation of  $\{\Omega_i\}_{i=1}^m$  is regarded as the permutation of  $\{T_j\}_{j=1}^n$ . Assume that  $\Omega_i$  is composed by  $T_{i_1}, T_{i_2}, \dots, T_{i_l}$ , where  $l = n\gamma_i$ ; then the subscript set  $\{i_1, i_2, \dots, i_l\}$  is a subset of  $\mathcal{K} = \{1, 2, \dots, n\}$  and  $\theta_{i_\xi} = \rho_i$ ,  $\xi = 1, 2, \dots, l$ . The perturbation between  $\Omega_i$  and  $\Omega_j$  allows us to rearrange the subscript sets of  $T_{i_\xi}$  and  $T_{j_\eta}$ , where  $\xi = 1, 2, \dots, l$  and  $\eta = 1, 2, \dots, r$ . For example, if  $T_{i_\xi}$  and  $T_{j_\eta}$  are exchanged after the perturbation, it follows that

$$\Omega_i^1 = \left( \bigcup_{\substack{\xi \neq \xi' \\ \xi \in \{1, 2, \dots, l\}}} T_{i_\xi} \right) \cup T_{j_{\eta'}}, \quad \Omega_j^1 = \left( \bigcup_{\substack{\eta \neq \eta' \\ \eta \in \{1, 2, \dots, r\}}} T_{j_\eta} \right) \cup T_{i_{\xi'}}.$$

We denote by  $\rho^k$  the density  $\rho$  with respect to  $\{\Omega_i^k\}_{i=1}^m$ , the  $k$ -th perturbation of  $\{\Omega_i\}_{i=1}^m$ . Obviously,  $\rho^k \in ad_\gamma(\Omega)$ , where

$$\Omega = \bigcup_{i=1}^m \Omega_i^k, \quad \|\Omega_i^k\| = \gamma_i \|\Omega\|, \quad i = 1, 2, \dots, m.$$

For simplification of notation, we set the least eigenvalue  $\lambda_1^k := \lambda_1(\rho^k(x))$  and the first eigenfunction  $u_1^k := u_1(\rho^k(x))$ , where  $\rho^k(x) \in ad_\gamma(\Omega)$ .

Based on the above analysis, we have the following conclusion:

**Theorem 2.1.** *The discrete problem (2.5) with the discrete constraint condition (2.7) exists at most  $N(n)$  different values of  $\Xi_1$ , where*

$$N(n) = C_n^{\gamma_1 n} C_{(1-\gamma_1)n}^{\gamma_2 n} C_{(1-\gamma_1-\gamma_2)n}^{\gamma_3 n} \cdots C_{\gamma_m n}^{\gamma_m n}, \quad \text{with } C_i^j = \frac{i!}{j!(i-j)!}.$$

*Proof.* We use the above assumption that the domain is divided into uniform rectangular elements  $\{T_j\}_{j=1}^n$ . We choose  $\gamma_i n$  elements from the divisions as  $\Omega_i$  and denote by  $I_i$  the set of the elements' subscript. Moreover, the elements of  $\Omega_i$  satisfy the constraint condition

$$\sum_{j \in I_i} \|T_j\| = \|\Omega_i\| = \gamma_i \|\Omega\|.$$

Obviously, there are  $C_n^{\gamma_1 n}$  different ways to select  $\gamma_1 n$  elements, which form  $\Omega_1$ . And, from the rest  $(1-\gamma_1)n$  elements, we have  $C_{(1-\gamma_1)n}^{\gamma_2 n}$  different ways to choose  $\gamma_2 n$  elements as  $\Omega_2$ . By analogy, we accordingly have  $C_{\gamma_m n}^{\gamma_m n}$  choices to choose  $\gamma_m n$  elements from the rest  $(1-\gamma_1-\gamma_2-\cdots-\gamma_{m-1})n = \gamma_m n$  ones, which form  $\Omega_m$ . Therefore, the number of different combination of  $\{\Omega_i = \bigcup_{j \in I_i} T_j\}_{i=1}^m$  is

$$N(n) = C_n^{\gamma_1 n} C_{(1-\gamma_1)n}^{\gamma_2 n} C_{(1-\gamma_1-\gamma_2)n}^{\gamma_3 n} \cdots C_{\gamma_m n}^{\gamma_m n}.$$

Note that once the  $\{\Omega_i\}_{i=1}^m$  is determined, so as  $\Theta$ . And  $\Xi_1$  and  $U_1$  are also determined. Consequently,  $\Xi_1$  exist at most  $N(n)$  different values. □

It is noted that if  $n \rightarrow \infty$ , so is  $N(n) \rightarrow \infty$ . By Theorem 2.1, we conclude that the least eigenvalue  $\Xi_1$  of the discrete problem (2.5) and (2.7) exists infinite different values, when  $n \rightarrow \infty$ . Therefore, we get a monotone decreasing subsequence of  $\Xi_1$  as follows:

**Theorem 2.2.** *The discrete problem (2.5) with the discrete constraint condition (2.7) possesses a monotonically decreasing sequence of  $\Xi_1^k$ , where  $\Theta^k \in AD_\gamma$ . Furthermore, the limit of this sequence exists as  $k \rightarrow \infty$ .*

*Proof.* Corresponding to  $\Theta^k \in AD_\gamma$  and  $\{\Omega_i^k\}_{i=1}^m$ , we denote by  $\Xi_1^k$  the least eigenvalue of (2.5) with the associated eigenfunction  $U_1^k$ . That is

$$\Xi_1^k = \frac{1}{\mathcal{R}(U_1^k, \Theta^k)},$$

where

$$\mathcal{R}(U, \Theta) = \sum_{i=1}^n \theta_i H_i(U).$$

We rearrange  $\{\theta_i^k\}_{i=1}^n$  as  $\theta_{s_1}^k \leq \theta_{s_2}^k \leq \cdots \leq \theta_{s_n}^k$  and the sequence  $H_i^k(U)$  as

$$H_{i_1}^k(U) \leq H_{i_2}^k(U) \leq \cdots \leq H_{i_n}^k(U),$$

where both  $\{s_1, s_2, \dots, s_n\}$  and  $\{i_1, i_2, \dots, i_n\}$  are the permutations of  $\mathcal{K} = \{1, 2, \dots, n\}$ . By Lemma 2.1, we get

$$\mathcal{R}(U^k, \Theta^k) \leq \sum_{j=1}^n \theta_{s_j}^k H_{i_j}^k(U).$$

With the pair  $(\theta_{s_j}^k, T_{i_j})$ , we introduce  $\Theta^{k+1}$  and  $\{\Omega_i^{k+1}\}_{i=1}^m$ , where

$$\Theta^{k+1} = [\theta_1^{k+1}, \theta_2^{k+1}, \dots, \theta_n^{k+1}], \quad \theta_{i_j}^{k+1} = \theta_{s_j}^k$$

and

$$\Omega_i^{k+1} = \bigcup_{i_j \in I_i} T_{i_j},$$

$I_i$  is the set of index  $i_j$  such that  $\theta_{i_j}^{k+1} = \rho_i$ . It immediately follows

$$\Xi_1^k = \frac{1}{\mathcal{R}(U_1^k, \Theta^k)} \geq \frac{1}{\mathcal{R}(U_1^k, \Theta^{k+1})} \geq \min_{\langle KU, U \rangle = 1} \frac{1}{\mathcal{R}(U, \Theta^{k+1})} = \Xi_1^{k+1}.$$

Therefore, there exists a monotonically decreasing sequence of  $\Xi_1^k$ .

In addition,  $\Theta > 0$ , and the mass matrix  $M_{ij}$  is symmetric and positive. Then

$$\Xi_1(\Theta) = \min_{\langle KU, U \rangle = 1} \frac{1}{\mathcal{R}(U, \Theta)} = \min_{\langle KU, U \rangle = 1} \frac{1}{\langle MU, U \rangle} > 0.$$

It implies that  $\Xi_1(\Theta)$  is lower bounded and its limit exists as  $k \rightarrow \infty$ . □

We now return to (2.9) and present the monotonically decreasing iteration method according to Theorem 2.2. We introduce  $\Theta^{old}, \Theta^{new}, U_1^{old}, U_1^{new}, \Xi_1^{old}$  and  $\Xi_1^{new}$ , where the superscript 'old' refers to the data in the previous iteration step and 'new' means the data updated. Consequently,  $\Xi_1^{old} \geq \Xi_1^{new}$ , because

$$\begin{aligned} \Xi_1^{old} &= \frac{1}{\mathcal{R}(U_1^{old}, \Theta^{old})} \geq \frac{1}{\mathcal{R}(U_1^{old}, \Theta^{new})} \geq \min_{\langle KU, U \rangle = 1} \frac{1}{\mathcal{R}(U, \Theta^{new})} \\ &= \frac{1}{\mathcal{R}(U_1^{new}, \Theta^{new})} = \Xi_1^{new}. \end{aligned}$$

We list the monotonically decreasing algorithm as follows:

- 
- initial guess for  $\Theta^{(0)} \in AD_\gamma$
  - do while not optimal ( $\Theta^{(j+1)} \neq \Theta^{(j)}$ )
    - compute  $U^{(j)}$ , the minimizer of  $U \mapsto \mathcal{R}(U, \Theta^{(j)})$
    - compute  $H_i(U^j)$  according to (2.8)
    - update  $\Theta^{(j)} \rightarrow \Theta^{(j+1)}$ , according to  $H_i(U^j)$
-

**Remark 2.1.** From the presented algorithm, it can be observed that if for any  $i \in \mathcal{K} = \{1, 2, \dots, n\}$  such that  $\rho(T_i) = \rho_j$ , then there exist two constants  $\nu_{j-1}$  and  $\nu_j$  such that  $\nu_{j-1} < H_i(U) \leq \nu_j$ . More precisely,

$$\begin{aligned} \rho(T_i) = \rho_1 &\Rightarrow 0 < H_i(U) \leq \nu_1, \\ \rho(T_i) = \rho_2 &\Rightarrow \nu_1 \leq H_i(U) \leq \nu_2, \\ &\vdots \\ \rho(T_i) = \rho_m &\Rightarrow \nu_{m-1} \leq H_i(U) \leq \nu_m, \end{aligned} \tag{2.10}$$

where  $i = 1, 2, \dots, n$ .

If  $m = 2$ , (2.10) implies that there exists a constant  $\nu$  such that

$$\begin{cases} \rho(x) = \rho_1, & \text{if } H_i(U) \leq \nu, \\ \rho(x) = \rho_2, & \text{if } H_i(U) \geq \nu. \end{cases} \tag{2.11}$$

Recalling (1.8), we note that (2.11) is the equivalence form of it. In fact, from  $H_i(U) = \int_{T_i} u_1^2 dx$ , it obviously follows

$$H_i(U) < \nu \Leftrightarrow u(x) < \nu'.$$

### 3 Numerical results

In this section we present some numerical experiments of the monotone algorithm for the eigenvalue optimization problems in the two-dimensional shape design. To be more specific, a discretization eigenvalue problem is obtained by the finite element discretization. Based on the least eigenvalue and its associated eigenfunction,  $H_i(U)$  ( $i = 1, 2, \dots, n$ ) are sorted as an increasing sequence. Then  $\Xi_1$  and  $\rho$  are updated following the sorted sequence  $H_i(U)$  ( $i = 1, 2, \dots, n$ ). And this procedure continues until the stop criterion is satisfied. The whole algorithm is coded by ourselves, which includes the finite element discretization and the sequence sorting, as well as the operations of the large scale sparse matrix. The computations of eigenvalue and eigenfunction are carried out by the *eigs* function found in MATLAB [24]. Throughout the numerical results we always adopt the stop criterion  $\Theta^{(j+1)} = \Theta^{(j)}$ .

**Example 3.1.** We first consider the structural vibration control problem of a drumhead in a rectangular domain  $\Omega = [0, 1] \times [0, 1.5]$ . The densities of two materials are  $\rho = 1, 2$  and presented by white and black respectively (see Fig. 2). We suppose the two materials have equal areas, i.e.,  $\gamma_{white} = \gamma_{black} = 1/2$ .

Our goal is to predict the minimum of the least eigenvalue  $\lambda_1$ . The authors of [16] have investigated it only in the mesh sizes  $\Delta x = \Delta y = 0.025$  ( $40 \times 60$  mesh grids, see [16] Fig. 5).

Table 1: A comparison of our numerical prediction with existing result given in [16] when the densities  $\rho_1=1$  and  $\rho_2=2$  have the same half area. [16] has only listed the result in the mesh sizes  $1/40 \times 1/40$  with 200 iterative steps. We respectively compute five cases of different mesh sizes, where the minimal sizes  $\Delta x = \Delta y = 0.005$  are 25 times smaller than those in [16].

| the mesh sizes<br>$\Delta x = \Delta y = h$ | monotone algorithm |             | method in [16]    |             |
|---|--------------------|-------------|-------------------|-------------|
|   | $\min \lambda_1$   | iteration # | $\min \lambda_1$  | iteration # |
| $h = 1/40$                                  | 7.3749             | 3           | a little blew 7.4 | 200         |
| $h = 1/80$                                  | 7.3713             | 4           |                   |             |
| $h = 1/120$                                 | 7.3707             | 4           |                   |             |
| $h = 1/160$                                 | 7.3705             | 4           |                   |             |
| $h = 1/200$                                 | 7.3704             | 4           |                   |             |

In Table 1, we list our newly computed results together with the existing result for a comparison. 'A little blew 7.4' on ' $\min \lambda_1$ ' (the right column) is the minimum of the least eigenvalue  $\lambda_1$  estimated in [16]. The ' $\min \lambda_1$ ' on the left column are our results for the different mesh sizes. Especially, using the same  $40 \times 60$  mesh grids, our algorithm finds  $\min \lambda_1 = 7.3749$  in the third iterative step which is greatly less than 200-th step in [16]. Even though we take smaller mesh sizes and more spatial grid points, our algorithm converges still fast and obtains a stable minimum of  $\lambda_1$  in a few iterative steps.

On the other hand, we note a fact that the minimum of  $\lambda_1$  decreases as the mesh grids increase. This shows the sensitivity of  $\min \lambda_1$  to the choice of the mesh sizes. In Table 1, the difference between  $\min \lambda_1 = 7.3704$  and  $\min \lambda_1 = 7.3749$  is  $|\Delta \lambda_1| = 4.5 \times 10^{-3}$ . The mesh grids with respect to these two cases of  $\min \lambda_1$  are respectively  $200 \times 300$  and  $40 \times 60$ , where the mesh sizes of the former are equal to 25-time refining of the latter. However, the more times the mesh sizes refines, the less serious the sensitivity is. When the mesh grids change from  $40 \times 60$  to  $80 \times 120$ ,

$$|\Delta \lambda_1| = |7.3749 - 7.3713| = 3.6 \times 10^{-3}.$$

From  $160 \times 240$  to  $80 \times 120$ , the refinement times of the mesh sizes are the same as that in the case from  $80 \times 120$  to  $40 \times 60$ , whereas

$$|\Delta \lambda_1| = |7.3705 - 7.3713| = 8.0 \times 10^{-4}.$$

Hereafter, we always adopt  $200 \times 300$  mesh grids to simulate the numerical results unless otherwise stated. Certainly, we may further refine the mesh sizes if necessary and get a smaller  $\min \lambda_1$ .

Fig. 2 shows the profiles of  $\rho$  in  $200 \times 300$  mesh grids. The left subgraph in Fig. 2 shows the initial guess of the density distribution. The right subgraph is the situation of  $\rho$  in which the algorithm gets a stable minimum  $\lambda_1$ . Correspondingly, we may observe the values of  $\lambda_1$  in Fig. 3. In the fourth iteration,  $\min \lambda_1 = 7.3704$  is found.

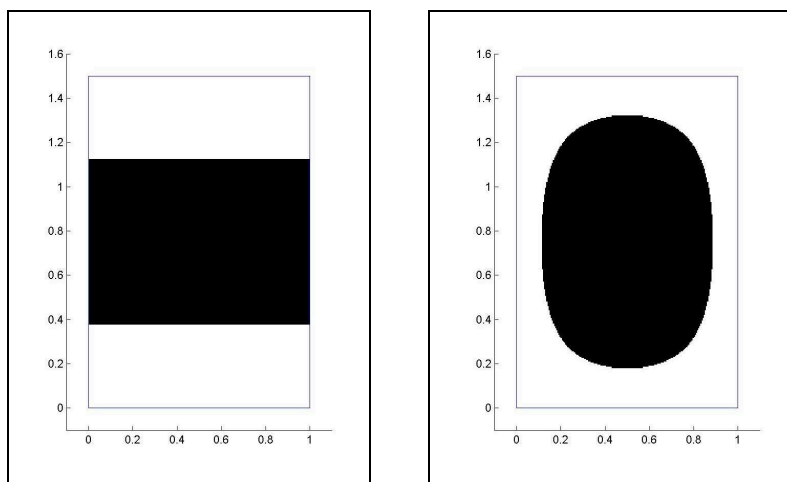


Figure 2: The profiles of the density distribution  $\rho$  in  $200 \times 300$  mesh grids.  $\Omega = [0,1] \times [0,1.5]$ ,  $\rho_1 = 1$  (in the subdomain of white color),  $\rho_2 = 2$  (in the black color) and  $\gamma_1 = \gamma_2 = 1/2$ . Left: the initial density distribution. Right: the density distribution at the stage of  $\min \lambda_1 = 7.3704$ .

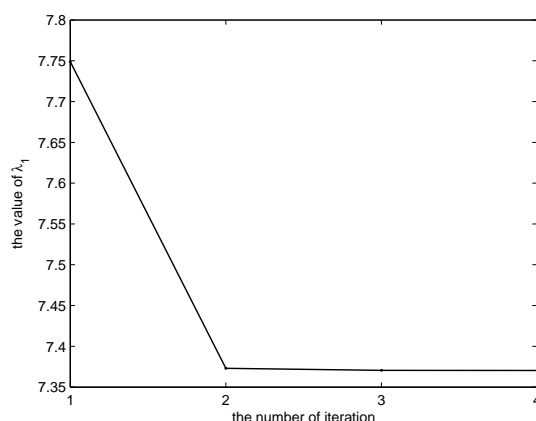


Figure 3: The evolution of  $\lambda_1$ . The algorithm finds the minimum of  $\lambda_1$  in the fourth iteration.  $\lambda_1$  at four stages are respectively 7.7489, 7.3730, 7.3705 and 7.3704.

**Example 3.2.** This problem is a drumhead with three material densities. Suppose that  $\Omega = [0,1] \times [0,1.5]$  and three material densities are  $\rho = 1$  (presented by white color),  $\rho = 2$  (red color) and  $\rho = 3$  (green color) respectively (see Fig. 4). Moreover, three materials have equal areas,  $\gamma_{white} = \gamma_{red} = \gamma_{green} = 1/3$ . The subgraph in the top-left corner of Fig. 4 shows the initial guess of the density distribution.

Fig. 4 also shows the profiles of  $\rho$  in other five iterations. Note that the algorithm finds the minimum of  $\lambda_1 = 5.1061$  in the 6-th iteration. Moreover, the first eigenfunction  $u_1$  is displayed in the bottom subgraph of Fig. 4. The contour map with two contour lines is depicted on the right side of the subgraph of  $u_1$ , where the contour lines are

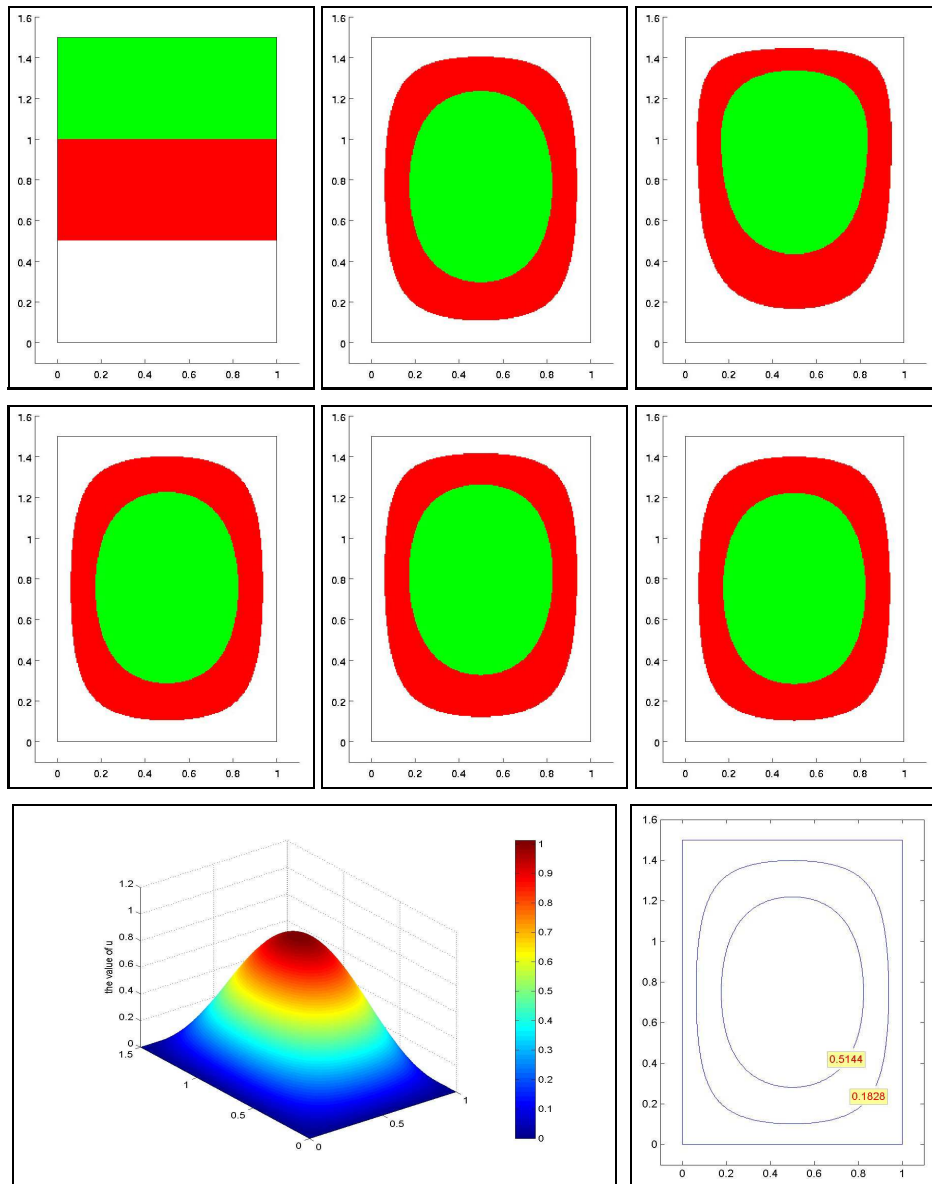


Figure 4: The evolution profiles of the density distribution  $\rho$  and the corresponding first eigenfunction  $u_1$  in  $200 \times 300$  mesh grids ( $\Omega = [0,1] \times [0,1.5]$ ,  $\rho_1 = 1$ ,  $\rho_2 = 2$ ,  $\rho_3 = 3$  and  $\gamma_1 = \gamma_2 = \gamma_3 = 1/3$ ). Top: from the left to the right, the profiles of  $\rho$  in the iteration  $n = 1, 2, 3$ ; Middle: from the left to the right, the profiles of  $\rho$  in the iteration  $n = 4, 5, 6$ ; Bottom: the left subgraph is  $u_1$  with the density distribution  $\rho$  in the sixth iteration and the corresponding eigenvalue  $\min \lambda_1 = 5.1061$ . Two contour lines  $u_1 = 0.1828$  and  $u_1 = 0.5144$  are displayed in the right subgraph.

$u_1 = 0.1828$  and  $u_1 = 0.5144$  respectively. It can be observed that the contour lines do almost coincide with the boundaries among the difference colors, which are listed in the subgraph of the profile  $\rho$ , i.e., in the sixth subgraph of Fig. 4. We take 0.1828 and 0.5144

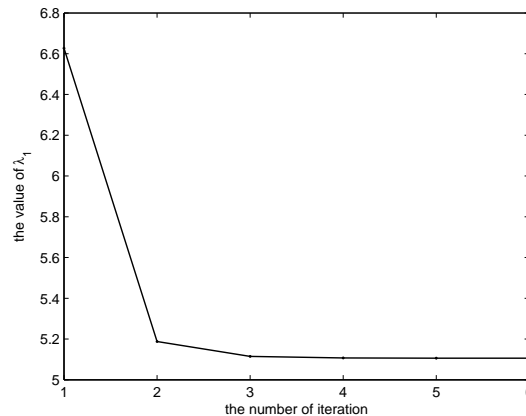


Figure 5: The evolution of  $\lambda_1$ . The algorithm finds the minimum of  $\lambda_1 = 5.1061$  in the sixth iteration.  $\min \lambda_1$  in the fourth and the fifth iteration are respectively 5.1072 and 5.1063.

as the approximations of  $v_1$  and  $v_2$ , respectively. Let  $v_3 = \max u_1$  and we have the formula (2.10) for three densities

$$\begin{aligned} \Omega_1 &= \bigcup_i \{T_i \mid \rho(T_i) = 1\} (\text{white subdomain}) \Rightarrow 0 < H_i(U) \leq v_1, \\ \Omega_2 &= \bigcup_i \{T_i \mid \rho(T_i) = 2\} (\text{red subdomain}) \Rightarrow v_1 \leq H_i(U) \leq v_2, \\ \Omega_3 &= \bigcup_i \{T_i \mid \rho(T_i) = 3\} (\text{green subdomain}) \Rightarrow v_2 \leq H_i(U) \leq v_3. \end{aligned}$$

On the other hand, it is observed that the three subgraphs of  $\rho$  in the middle of Fig. 4 do not make such a difference. This illustrates that  $\lambda_1$  in the fourth and the fifth iterations have approached the minimum of  $\lambda_1$ . Correspondingly, we may find the values of  $\lambda_1$  in Fig. 5 and confirm this by  $\lambda_1 = 5.1072$  ( $n = 4$ ),  $5.1063$  ( $n = 5$ ),  $5.1061$  ( $n = 6$ ).

**Example 3.3.** Suppose that the drumhead includes much more different materials. What happens about the minimization of the least eigenvalue and the process of minimizing? The domain is still a rectangular domain  $\Omega = [0, 1] \times [0, 1.5]$ , like that in Example 3.2. Each of the ten densities,  $\rho_i = i$  ( $i = 1, \dots, 10$ ), is respectively presented by one of ten colors in Fig. 6, where  $\rho_1$  is presented by white color and  $\rho_{10}$  by green color. And  $\gamma_1 = \gamma_2 = \dots = \gamma_{10} = 1/10$ .

Fig. 6 shows the evolution of the density distribution  $\rho$ . The nine different stages of  $\rho$ , i.e., the iteration from  $n = 1$  to 9, are displayed. The subgraph in the top-left corner of Fig. 6 shows the initial guess of the density distribution. Through nine iterations, the algorithm finds the minimum of  $\lambda_1$ , which is 1.6749 (see Fig. 8). Moreover, the eigenfunction  $u_1$ , with respect to the minimum of  $\lambda_1$  and the corresponding  $\rho$ , is displayed in the left subgraph of Fig. 7. It is observed that the contour lines  $u_1 = 0.0190, 0.0483, 0.0845,$

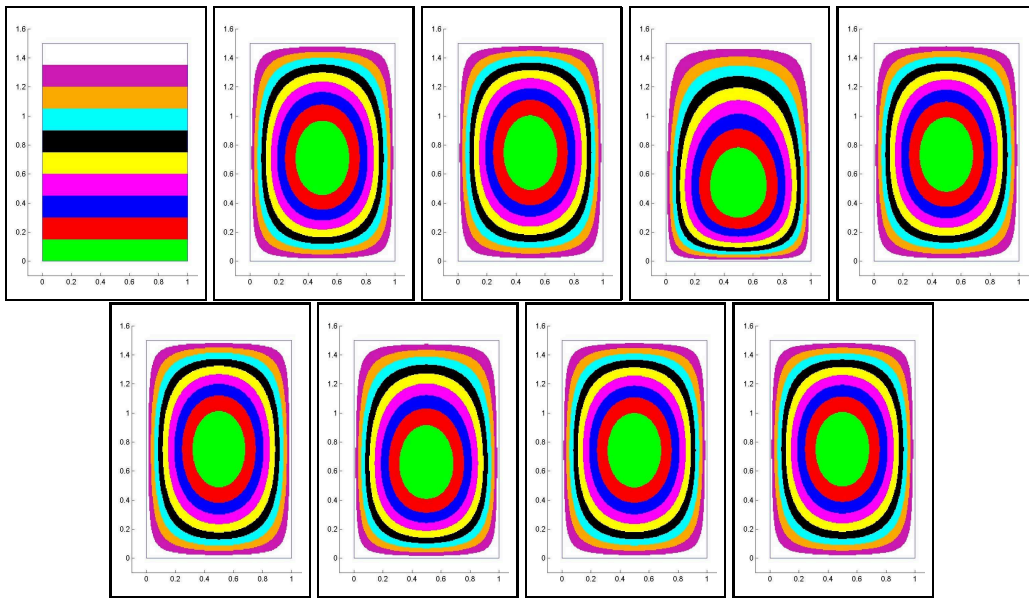


Figure 6: The evolution profiles of the density distribution  $\rho$  in  $200 \times 300$  mesh grids ( $\Omega = [0,1] \times [0,1.5]$ ,  $\rho_i = i$ , ( $i = 1, \dots, 10$ ) and  $\gamma_1 = \dots = \gamma_{10} = 1/10$ ). Top: from the left to the right, the profiles of  $\rho$  in the iteration of  $n = 1, 2, 3, 4, 5$ ; Bottom: from the left to the right, the profiles of  $\rho$  in the iteration of  $n = 6, 7, 8, 9$ .

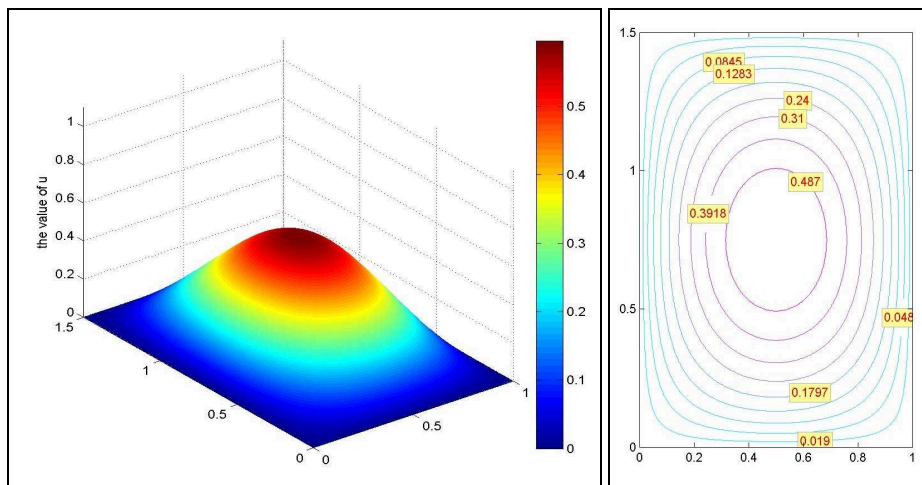


Figure 7: The profiles of the solution  $u$  and the corresponding contour lines in  $200 \times 300$  mesh grids ( $\Omega = [0,1] \times [0,1.5]$ ,  $\rho_i = i$ , ( $i = 1, \dots, 10$ ) and  $\gamma_1 = \dots = \gamma_{10} = 1/10$ ). Left: the first eigenfunction  $u_1$  in the minimum of  $\lambda_1$  is displayed. Right: Nine contour lines are located in  $u_1 = 0.0190, 0.0483, 0.1283, 0.2400, 0.3100, 0.3918, 0.4870$  respectively. Compared with the boundaries among different colors, these contour lines almost coincide with them.

0.1283, 0.1797, 0.2400, 0.3100, 0.3918, 0.4870 in the right subgraph of Fig. 7 are almost the boundaries among the different colors. Therefore, we may confirm that there are indeed  $v_i$  ( $i = 1, \dots, 10$ ) such that (2.10) is satisfied.

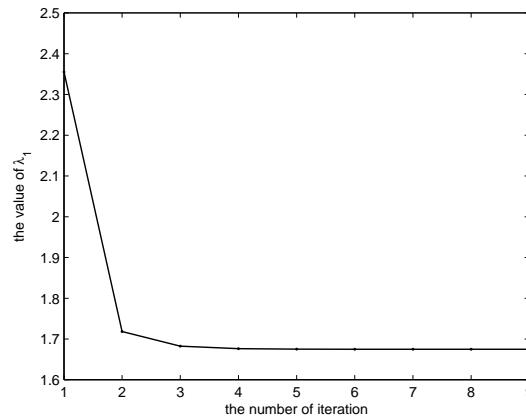


Figure 8: The evolution of  $\lambda_1$ . The algorithm finds the minimum of  $\lambda_1$  in the ninth iteration.  $\lambda_1$  decreases from 2.3554 in the first iteration to 1.6749 in the ninth iteration.

**Example 3.4.** We now consider the situation that the domain is a nonconvex region, a L-shape domain. Suppose  $\Omega = [0,1] \times [0,1] \setminus [0,1/2] \times [0,1/2]$ , That is a square domain cutting off the one-fourth region in the bottom-left corner. We use three different colors to present three densities of the materials (see Fig. 9), the same as in Example 3.2 the case of the rectangular region with three densities. Moreover, three materials have equal areas, i.e.,  $\gamma_i = 1/3$ , ( $i = 1, 2, 3$ ).

We choose  $\Delta x = \Delta y = 1/200$  and there are 30,000 rectangular elements over the L-shape domain. The subgraph in the top-left corner of Fig. 9 shows the initial guess of density distribution. Following it, eight subgraphs in Fig. 9 are the profiles of the density distribution  $\rho$  in the iterations from  $n = 2$  to 9 respectively. And the least eigenvalue  $\lambda_1$  decreases from 4.3181 to 3.3958.

In the left subgraph of Fig. 10, the first eigenfunction  $u_1$  is displayed with respect to the minimum of  $\lambda_1$  and the corresponding  $\rho$ . The right subgraph of Fig. 10 demonstrates the contour lines  $u = 0.0960, 0.3251$  respectively. Note that each contour line do almost coincide with the boundary between two different colors. Hence we may confirm that in a nonconvex domain, such as L-shape, there also exist  $v_i$  ( $i = 1, 2, 3$ ) such that piecewise conditions (2.10) are satisfied.

In Table 2, we present the corresponding values of the minimal  $\lambda_1$  for the different mesh sizes and the different  $\{\gamma_i\}_{i=1}^3$ . The first column of Table 2 shows that in the case of  $\gamma_i = \frac{1}{3}$ ,  $i = 1, 2, 3$ , if the mesh is refined 5-time in  $x$ -direction and  $y$ -direction respectively, the corresponding  $\min \lambda_1$  may have a big change

$$\Delta \lambda_1 = |3.4080 - 3.3958| = 1.22 \times 10^{-2}.$$

In the second and the third columns, we fix  $\gamma_1 = \frac{1}{3}$  and change  $\gamma_2$  and  $\gamma_3$ . The difference of  $\min \lambda_1$  caused by the mesh refinement is

$$\Delta \lambda_1 = |3.2902 - 3.2786| = 1.16 \times 10^{-2}$$

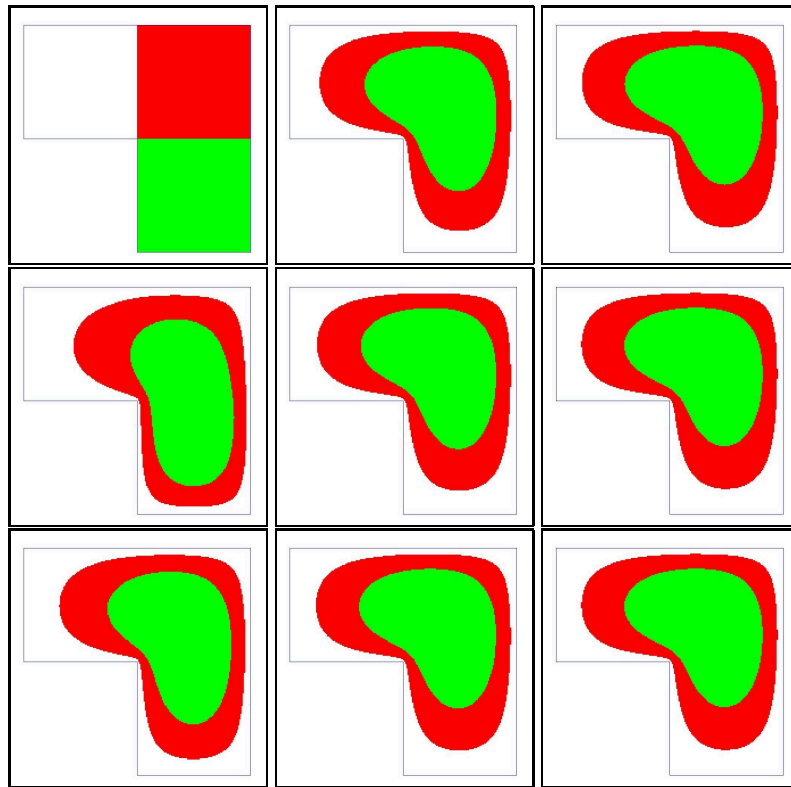


Figure 9: The evolution profiles of the density distribution  $\rho$  in L-shape with 30,000 elements. ( $\Omega = [0,1] \times [0,1] \setminus [0,1/2] \times [0,1/2]$ ,  $\rho_i = i$ , ( $i=1,2,3$ ) and  $\gamma_1 = \gamma_2 = \gamma_3 = 1/3$ ). Top: from the left to the right, the profiles of  $\rho$  in the iteration of  $n=1, 2, 3$ ; Middle: from the left to the right, the profiles of  $\rho$  in the iteration  $n=4, 5, 6$ . Bottom: from the left to the right, the profiles of  $\rho$  in the iteration of  $n=7, 8, 9$ .

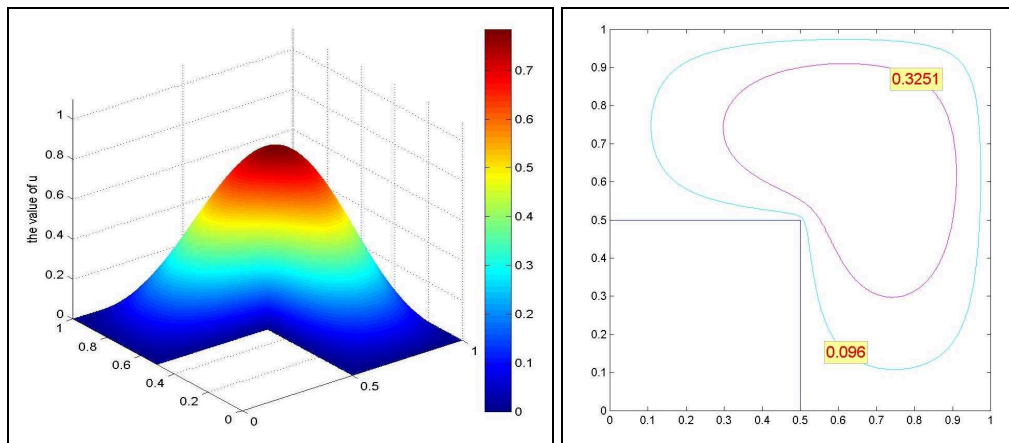


Figure 10: The profile of the solution  $u$  and the corresponding contour lines in L-shape with 30,000 mesh grids. ( $\Omega = [0,1] \times [0,1] \setminus [0,1/2] \times [0,1/2]$ ,  $\rho_i = i$ , ( $i=1,2,3$ ) and  $\gamma_1 = \gamma_2 = \gamma_3 = 1/3$ ). Left: the first eigenfunction  $u_1$  in the minimum of  $\lambda_1$  is displayed. Right: Two contour lines are located in  $u_1 = 0.0960, 0.3251$  respectively. Compared with the boundaries among different colors, these contour lines almost coincide with them.

Table 2: The minimum of the least eigenvalue are obtained, for different mesh sizes and different  $\gamma_i$ , via the monotone algorithm when the materials have three different densities and the domain is the L-shape domain.

| the mesh size<br>$\Delta x = \Delta y = h$ | $\gamma_1 = \gamma_2 = \gamma_3 = 1/3$ |                  | $\gamma_1 = 1/3, \gamma_2 = 1/6, \gamma_3 = 1/2$ |                  | $\gamma_1 = 1/3, \gamma_2 = 7/12, \gamma_3 = 1/12$ |                  |
|--|--|------------------|--|------------------|--|------------------|
|  | $\min \lambda_1$                       | iteration number | $\min \lambda_1$                                 | iteration number | $\min \lambda_1$                                   | iteration number |
| $h = 1/40$                                 | 3.4080                                 | 6                | 3.2902   | 6                | 4.1143   | 7                |
| $h = 1/80$                                 | 3.3991                                 | 8                | 3.2817   | 7                | 4.1028   | 7                |
| $h = 1/120$                                | 3.3970                                 | 9                | 3.2797   | 8                | 4.1003   | 8                |
| $h = 1/160$                                | 3.3962                                 | 9                | 3.2790   | 9                | 4.0993   | 10               |
| $h = 1/200$                                | 3.3958                                 | 9                | 3.2786   | 9                | 4.0988   | 13               |

and

$$\Delta \lambda_1 = |4.1143 - 4.0988| = 1.55 \times 10^{-2}$$

in these two columns respectively. All three differences of  $\min \lambda_1$  in Table 2 are a little bigger than that in Example 3.1 where  $\Delta \lambda_1 = 4.5 \times 10^{-3}$ . In some sense, this shows that the more densities are the more sensitive to the choice of the mesh sizes. We also note that decreasing the greatest density  $\gamma_3$  does cause the bigger  $\min \lambda_1$  and the more iteration numbers.

From Examples 3.3 and 3.4 (see Figs. 6 and 9), we observe that the highest density (the green color) assembles at the center of the domain. The lower the density is, the further away from the center it is. This well agrees with the argument of [13] which places the high density in the center and fills the remains by the low density. On the other hand, the profiles of the densities keep a certain symmetry even though the initial densities do not. The profile of  $\rho$  in Example 3.3 is symmetric with both  $x$ -axis and  $y$ -axis. Moreover,  $\rho$  in Example 3.4 is symmetric with the line  $y = x$ .

## 4 Conclusion

In this paper, we propose a monotonically decreasing approach to minimize the least eigenvalue in the shape design problem of multi-density inhomogeneous material. Its motivation is not the same as that of [5]. The key point of [5] is to approach the level-set line  $\Gamma$ . The main idea of the monotone algorithm in this paper is the sorting order. Based on (1.6), the density  $\rho$  is chosen from  $ad_\gamma(\Omega)$  such that  $\mathcal{R}(u, \rho)$  attains its extremum. This is also different from the level set method in [16] where tracking the front is important. Compared with the level set method, the monotone algorithm converges faster and obtain a stable minimum of  $\lambda_1$  in fewer iterations. Furthermore, the examples in this paper have illustrated that the discretization mesh sizes are very sensitive to the computation of  $\min \lambda_1$ . Hence, we adopt  $200 \times 300$  mesh grids to accurately simulate the numerical results, which is 25-time more than the mesh grids in [16].

As we state in the section of Introduction, we only focus on the first optimal problem (i), i.e.,  $\min \lambda_1$ , rather than dealing with all three optimal problems as does the level set method in [16]. Although the monotone algorithm can not be assured of reaching a global minimum, it has a significant speed-up. Moreover, this method is independent of the initial guess, the complexity of the domain, and the number of different material densities. The numerical examples are also presented to demonstrate the efficiency and accuracy of the monotone algorithm. Furthermore, it can be observed that the numerical results agree with the argument of [13] which has been strictly proved in the case of one dimensional  $\Omega$ .

## Acknowledgments

We are grateful to Steven J. Cox for providing his paper. We have benefited from the results in his paper. This research is supported by the Chinese National Science Foundation (No. 10871179), the National Basic Research Programme of China (No. 2008CB717806) and Specialized Research Fund for the Doctoral Program of Higher Education of China (SRFDP No. 20070335201).

## References

- [1] G. Allaire, S. Aubry and F. Jouve, Eigenfrequency optimization in optimal design, *Comp. Meth. Appl. Mech. Eng.* 190 (2001) 3565-3579.
- [2] J.W.S. Baron Rayleigh, *The Theory of Sound* (Macmillan, London, 1877-1878), 2nd ed. (1894), New York, 1945.
- [3] M.P. Bendsoe, *Optimization of Structural Topology, Shape and Material*, Springer-Verlag, Berlin, 1997.
- [4] M.P. Bendsoe and C.A. Mota Soares, *Topology Design of Structures*, Kluwer Academic, Dordrecht, 1993.
- [5] S.J. Cox, The two phase drum with the deepest bass note, *Japan J. of Industrial and Applied Math.*, 8 (1991) 345-355.
- [6] S.J. Cox, Extremal eigenvalue problems for the Laplacian, *Recent Advances in PDE*, Proceedings, M. Herrero and E. Zuazua eds., Masson, 1993.
- [7] S.J. Cox and J. McLaughlin, Extremal eigenvalue problems for composite membranes, I and II, *Appl. Math. Optimizat.* 22 (1990) 153-167, 169-187.
- [8] S.J. Cox and P. Uhlig, Where Best to hold a drum fast, *SIAM Review*, 45 (2003) 75-92.
- [9] J.E. Dennis and R. B. Schnabel, *Numerical Methods for Unconstrained Optimization and Nonlinear Equations*, SIAM, Philadelphia, 1996.
- [10] B.C. Faber, dass unter allen homogenen Membrane von gleicher Fläche und gleicher Spannung die kreisförmige die tiefsten Grundton gibt, *Sitzungsberbayer. Akad. Wiss., Math.-Phys. Munich*, 169-172, 1923.
- [11] E. Haber, A multilevel, level-set method for optimizing eigenvalues in shape design problems, *J. Comput. Phys.*, 198 (2004) 518-534.
- [12] E. Krahn, über eine von Rayleigh formulierte Minimaleigenschaft des Kreises, *Math. Ann.*, 94 (1925) 97-100.

- [13] M.G. Krein, On certain problems on the maximum and minimum of characteristic values and on the Lyapunov zones of stability, *AMS Translations Ser.*, 2 (1955) 163-187.
- [14] A.S. Lewis, The mathematics of eigenvalue optimization, *Mathematical Programming*, 97 (2003) 155-176.
- [15] A.S. Lewis and M.L. Overton, Eigenvalue optimization, *Acta Numer.*, 5 (1996) 149-190.
- [16] S. Osher and F. Santosa, Level set methods for optimization problems involving geometry and constraints I. frequencies of a two-density inhomogeneous drum, *J. Comput. Phys.*, 171 (2001) 272-288.
- [17] S. Osher and J. Sethian, Front propagation with curvature-dependent speed: Algorithms based on Hamilton-Jacobi formulations, *J. Comput. Phys.* 79 (1988) 12-49.
- [18] M.L. Overton, Large-scale optimization of eigenvalues, *SIAM J. Optim.*, 2 (1992) 88-120.
- [19] R. Pedrosa, Stability of optimal composite membranes, *International Research Experience for Students (IRES)-Campinas, SP, Brazil, 2006.*
- [20] W. Proskurowski, On the numerical solution of the eigenvalue problem of the laplace operator by a capacitance matrix method, *Computing*, 20 (1978) 139-151.
- [21] G.I.N. Rozvany, *Topology Optimization in Structural Mechanics*, Springer-Verlag, New York, 1997.
- [22] L. Rudin, S. Osher and E. Fatemi, Nonlinear total variation based noise removal algorithms, *Physica D*, 60 (1992) 259-268.
- [23] A. Shapiro, M.K.H. Fan, On eigenvalue optimization, *SIAM J. Optim.*, 5 (1995) 552-569.
- [24] The Mathworks Inc., *Matlab User's Guide*, version 7, The Mathworks Inc., Natick, MA, 2004.
- [25] H. Zhao, T. Chan, B. Merriman and S. Osher, A variational level set approach to multiphase motion, *J. Comput. Phys.*, 127 (1996) 179-195.